Journal of
Ship&Ocean
Technology

SOTECH Vol. 7, No. 2, pp. 1∼19, 2003

Unified Theory for the Radiation Problem of Multiple Slender Bodies

Yong-Hwan Kim[1]

[1]Department of Ocean Engineering, MIT, Cambridge, Massachusetts, USA;
E-mail: ykim@vfrl.mit.edu

Abstract

This paper introduces a unified theory for the radiation problem of adjacent multiple floating bodies. The particular case of interest is the multiple slender bodies that their centerlines are parallel. The infinite- and finite-depth unified theories for the single-body problem are extended to solve each sub-problem of multiple bodies. The present method is valid for deep water and moderate water depth, and applicable for individually floating bodies as well as multimaran-type vehicles. For the validation of the present method, the heave and pitch hydrodynamic coefficients for two adjacent ships are compared with the results of a three-dimensional method, and an excellent agreement is shown. The application includes the hydrodynamic coefficients and motion RAOs of four trimarans which have different longitudinal and transverse arrangements for sidehulls.

Keywords: multi-body problem, unified theory, slender-body approach, ship motions

1 Introduction

Wave interaction between multiple adjacent floating or fixed bodies is important in the design and operation of ships and offshore structures. The strength of wave interaction is critically dependent on the distance between adjacent bodies, and the body geometry is also involved. As the bodies approach closer, the hydrodynamic interaction becomes more profound.

The interaction among multiple cylinders is a practical problem related to the design of offshore platforms. An array of vertical axisymmetric cylinders was studied by Spring and Monkmeyer (1974), taking into account exact linear free surface interaction. For non-axisymmetric multiple cylinders, many studies including Ohkusu (1974), and Kagemoto and Yue (1985), Emmerhoff and Sclavounos (1996) were carried out by approximating the hydrodynamic interaction, and most studies assumed the bodies far apart. Recently, the importance of trapped modes in the design of offshore structures supported by vertical cylindrical bodies was brought by Maniar and Newman (1997). In these studies, the diffraction problem was a major concern.

The hydrodynamic interaction among multiple floating marine vehicles is also critical in their operational aspect. Such examples are the wave interaction between twin hulls of catamaran-type ships (Lee 1976), and two adjacent bodies (ship-ship or ship-platform) in on-loading or off-loading condition (Kim and Fang 1985, Fang and Kim 1986). Recently, as the Floating-Production-Offloading-Storage (FPSO) system is getting popular for oil extraction in deep sea, the wave interaction between FPSOs and shuttle tankers is of great interest for safe operation.

Numerical solutions of the associated linear or nonlinear boundary value problem can be obtained by a three-dimensional method, especially using a frequency-domain approach (e.g. WAMIT). The general manner of the frequency-domain approach is to solve the problem separately for each body and combine these solutions. Today, the time-domain approach takes advantage of the dramatic development of computing resources. The time-domain programs, e.g. LAMP (Lin and Yue 1990) and SWAN (Nakos et al 1993), have many advantages in its application and extension to engineering problems, therefore these are also applicable for the multi-body problem. Nevertheless, the application of a numerical method for multiple bodies is still expensive, especially for the radiation problem of multiple floating bodies.

The present study considers the radiation problem of multiple floating bodies by a classical technique, concentrating on the particular case of parallel slender bodies. When a body is enough slender that the order of longitudinal disturbance is much smaller than that of transverse disturbance, a slender-body theory is a powerful tool to obtain an approximated solution. The particular method applied in this study is unified theory. Unified theory is in the middle of strip theory and a three-dimensional panel method. This theory has an advantage as a slender-body theory, therefore sectional offset data can be directly applicable for the computation and the C.P.U. time is much less than any three-dimensional method. Moreover, unified theory includes the leading-order components of three-dimensional effect, so that its accuracy is comparable to a three-dimensional method.

Unified theory was introduced for the radiation and diffraction problems in deep water by Newman and Sclavounos (1978, 1980, 1985a). They extended and refined the previous slender-body theories, e.g. Korvin-Kroukovsky (1955), Salvesen et al (1970), and Ogilvie and Tuck (1969), and completed the foundation of unified theory. Recently, Kim and Sclavounos (1998) developed a finite-depth unified theory. For catamarans, the deep-water unified theory was applied by Breit and Sclavounos (1986), and Kashiwagi (1993). This theory has been also applied to the computation of the second-order forces (Kim and Sclavounos 1998, Kim 2000).

In this paper, a unified theory is introduced for general problems of multiple bodies, which is valid for both independently floating bodies and a single ship with multiple outriggers. Therefore, the approach method is slightly different with previous studies for catamarans. In order to observe the interaction of two bodies of catamarans, Breit and Sclavounos (1986) decomposed the linear velocity potential into demi-hull component and additional contribution from the other body, assuming the bodies are far enough apart to permit neglect of evanescent modes. In the case of Kashiwagi's study (1993), he applied the single-ship solution for the near-field solution, but the far-field solution was written as the line distributions of source and dipole along two centerlines. The present method assumes that the velocity potential is a sum of sub-problems as many as the number of the bodies. In each sub-problem, the linear motion is imposed for one specific body and no motion for the others. Then, the solution of each sub-problem includes the linear interaction among the bodies, which is proportional to the motion amplitude of the specified body.

This paper introduces two application examples, two adjacent Series 60 hulls and trimarans. Added-mass and damping coefficients are observed for heave and pitch motions, and both deep water and finite depth are considered. The computational results are compared with those of a three-dimensional panel method, showing an excellent agreement. The hydrodynamic coefficients

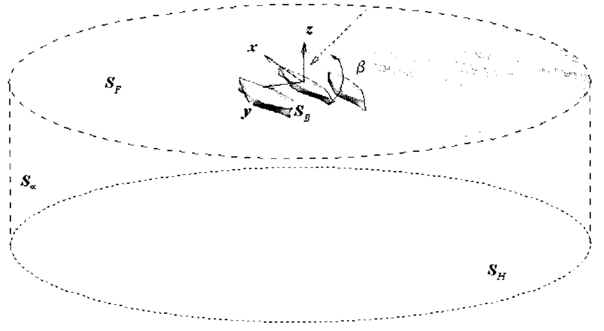

Figure 1: Coordinate system

and motion RAOs of trimarans are shown as an application for multimarans. For the trimarans, a single-ship approach is applied. Four different arrangements of two sidehulls are considered, and their results are compared.

2 Linear boundary value problem

Let's consider multiple freely-floating bodies in the presence of incoming waves with no forward speed. A Cartesian coordinate system in Figure 1 is fixed in space with the free surface taken at $z = 0$, the positive z-axis pointing upwards, and the positive x-axis pointing forwards. Assume that the bodies are under small amplitude harmonic motions in a monochromatic linear wave with frequency ω.
Then the body motion can be written as the following complex notation:

$$\xi_j^{(n)} = Re\{\xi_{j,0}^{(n)} e^{i\omega t}\} \tag{1}$$

where $\xi_{j,0}^{(n)}$ is the motion amplitude of $O(\varepsilon)$. $j = 1, 2, 3$ and $4, 5, 6$ correspond to the translational and rotational motions, and the superscript (n) is a body index. Now consider hydrodynamic force due to body motion only, i.e. radiation force. Using a series expansion with respect to the motion amplitudes, the hydrodynamic force of j mode on the (n)-th body can be written as follows:

$$F_j^{(n)} = F_j^{(n)}(\xi = 0, \bar{S}^{(n)}) + \sum_{m=1}^{M} \sum_{k=1}^{6} \xi_{k,0}^{(m)} \frac{\partial F_j^{(n)}}{\partial \xi_k^{(m)}} (\bar{S}^{(n)}) + O(\varepsilon^2) \tag{2}$$

where $\bar{S}^{(n)}$ is the mean surface of the (n)-th body, and M is the number of the bodies. The first expansion term is the force on the mean body position without motion. Obviously this term is zero. The second term is the linear force which is proportional to the motion amplitude $\xi_{k,0}^{(m)}$. $\partial F_j^{(n)}/\partial \xi_k^{(m)}$ indicates the force acting on the (n)-th body in j-direction due to unit-amplitude motion of the (m)-th body in k-direction. As the second series term remains linear, all the body motion except for the (m)-th body is restrained when $\partial F_j^{(n)}/\partial \xi_k^{(m)}$ is associated. The additional series are nonlinear terms and beyond our interest.

To obtain the force component $\partial F_j^{(n)}/\partial \xi_k^{(m)}$, the following boundary value problem for the velocity potential, $\Phi_{k,(m)}$, should be solved:

$$\nabla^2 \Phi_{k,(m)} = 0 \qquad \text{in fluid domain} \tag{3}$$

$$\frac{\partial \Phi_{k,(m)}}{\partial z} - v\Phi_{k,(m)} = 0 \qquad \text{on } z = 0 \tag{4}$$

$$\frac{\partial \Phi_{k,(m)}}{\partial n} = \begin{cases} i\omega n_k & \text{on the (m)-th body} \\ 0 & \text{on other bodies} \end{cases} \tag{5}$$

$$\frac{\partial \Phi_{k,(m)}}{\partial n} = 0 \qquad \text{on } z = -h \tag{6}$$

where $v = \omega^2/g$ and g, h, n_k are the gravitational constant, water depth, and the normal vector component, respectively. In addition, the radiation condition is essential in the far field.

The hydrodynamic force component is obtained by the integration of linear pressure. Adopting the concept of hydrodynamic coefficient, $\partial F_j^{(n)}/\partial \xi_k^{(m)}$ can be written as

$$\frac{\partial F_j^{(n)}}{\partial \xi_k^{(m)}} = -\rho \iint_{\xi(n)} i\omega \Phi_{k,(m)} n_j ds = \omega^2 A_{j,k}^{(n,m)} - i\omega B_{j,k}^{(n,m)} \tag{7}$$

where $A_{j,k}^{(n,m)}$ and $B_{j,k}^{(n,m)}$ are the added mass and damping coefficient, respectively. The total linear potential and hydrodynamic force are finally obtained by solving $6M$ sub-problems, i.e. $m = 1, .., M$ and $k = 1, .., 6$ in (3)~(6).

$$\Phi = Re\left\{ \sum_{k=1}^{6} \sum_{m=1}^{M} \xi_{k,0}^{(m)} \Phi_{k,(m)} e^{i\omega t} \right\} \tag{8}$$

$$F_j^{(n)} = Re\left\{ \sum_{k=1}^{6} \sum_{m=1}^{M} \xi_{k,0}^{(m)} \left\{ \omega^2 A_{j,k}^{(n,m)} - i\omega B_{j,k}^{(n,m)} \right\} e^{i\omega t} \right\} \tag{9}$$

When the bodies are connected like catamaran or trimaran, $\sum_{m=1}^{M} \left\{ \omega^2 A_{j,k}^{(n,m)} - i\omega B_{j,k}^{(n,m)} \right\}$ becomes the radiation force which is considered in the equation of motion.

3 Unified slender-body theory for $\partial F_j^{(n)}/\partial \xi_k^{(m)}$

This study concentrates on a particular case that all floating bodies are slender and their longitudinal centerlines are parallel. The bodies may have different body sizes and motion centers, but the distance between the bodies is limited to the order of body beam. This section describes an extension of the single-body unified theory to the multi-body problem, and heave and pitch motions are major interests.

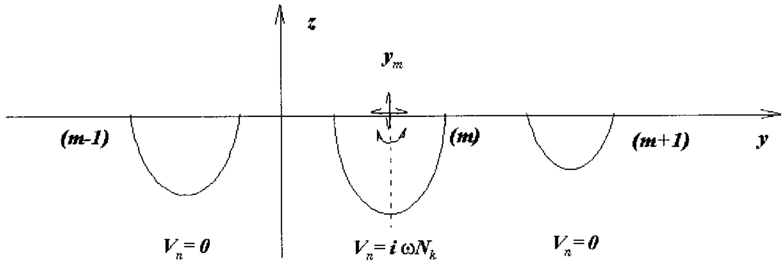

Figure 2: Sectional boundary value problem

3.1 Near-field solution

Let's consider a transverse cut of multiple bodies at an arbitrary x-coordinate, as shown in Figure 2. When the bodies are slender, the orders of the flow gradient near the body in the longitudinal and transverse directions are written as

$$O\left(\frac{\partial}{\partial x}\right) \ll O\left(\frac{\partial}{\partial y}, \frac{\partial}{\partial z}\right) \tag{10}$$

Then the boundary value problem of (3)$\sim$(6) is reduced to a two-dimensional problem. Now we will consider a sub problem that the (m)-th body is under the forced motion in k direction (Figure 2).

Let $\varphi_{k,(m)}$ the velocity potential which satisfies the two-dimensional boundary value problem including the body boundary condition,

$$\frac{\partial \varphi_{k,(m)}}{\partial n} = \begin{cases} i\omega N_k & \text{on the (m)-th body section} \\ 0 & \text{on other body sections} \end{cases} \tag{11}$$

where N_k is the normal vector component on the two-dimensional section. $\varphi_{k,(m)}$ is the solution that strip method uses. Despite satisfying all the boundary conditions, $\varphi_{k,(m)}$ is not a complete solution but a particular solution. Like a single-body case, the pure imaginary body boundary condition suggests that $\varphi_{k,(m)} + \varphi^*_{k,(m)}$ can be a homogeneous solution. Then the general solution $\phi_{k,(m)}$ is written as

$$\phi_{k,(m)}(x, y, z) = \varphi_{k,(m)} + C_{k,(m)}(x)(\varphi_{k,(m)} + \varphi^*_{k,(m)}) \tag{12}$$

where $C_{k,(m)}(x)$ is a complex constant which varies along x-axis, and the superscript $*$ means complex conjugate.

Similar to the single-body problem, the outer expansion of the near-field solution can be written as

$$\begin{aligned} \phi_{k,(m)} \approx & D_{k,(m)}(x) G_{2D}(y - y_m, z) \\ & + C_{k,(m)}(x)\{D_{k,(m)}(x) G_{2D}(y - y_m, z) + D^*_{k,(m)}(x) G^*_{2D}(y - y_m, z)\} \end{aligned} \tag{13}$$

where

$$D_{k,(m)}(x) = \sigma_{k,(m)}(x) + \mu_{k,(m)}(x)\frac{\partial}{\partial y} \tag{14}$$

$\sigma_{k,(m)}$ and $\mu_{k,(m)}$ are the strengths of the equivalent source and dipole located at $(y_m, 0)$. $G_{2D}(y, z)$ is the two-dimensional wave source (Wehausen and Laiton 1960, Eq.13.31 & 13.33). Equation (11) indicates that the outer expansion of the near-field solution has the flow behavior of point source and dipole. In the single-body problem which its geometry is symmetric on x-z plan, the source is enough to represent the heave and pitch (i.e. symmetric) motions, and also the dipole represents the sway and roll (i.e. anti-symmetric) motions. In the multi-body problem, both singularities should be considered as the interaction can have both behaviors. As a matter of fact, equation (12) and (13) have the same forms with the single-body case. This is an advantage of defining a sub problem.

In deep water, Newman (1978, VI-c) showed that, the leading-order solution of the antisymmetric mode is the particular solution. This case simplifies (11) as follows:

$$\begin{aligned}\phi_{k,(m)} \approx & [D_{k,(m)}(x) + C_{k,(m)}(x)\{\sigma_{k,(m)}(x) + \sigma^*_{k,(m)}(x)\}]G_{2D}(y - y_m, z) \\ & - C_{k,(m)}(x)\sigma^*_{k,(m)}(x)\{G_{2D}(y - y_m, z) - G^*_{2D}(y - y_m, z)\}\end{aligned} \tag{15}$$

This is valid up to $O(Kr)$ where K is the wave number and r is a distance from $(y_m, 0)$. For finite depth, more careful observation is needed. In particular, equation (13) is not exactly true in the limit case of shallow depth. This will be mentioned later.

Equation (12), corresponding to (15), is written as

$$\phi_{k,(m)} \approx \varphi_{k,(m)} + C_{k,(m)}(x)\left\{\varphi^{sym}_{k,(m)} + (\varphi^{sym}_{k,(m)})^*\right\} \tag{16}$$

where the superscript sym represents symmetric component.

3.2 Far-field solution

The solution in the far field located at a radial distance comparable to the body length takes the form of the single body problem, so that it can be written as a line distribution of the three-dimensional wave source and dipole along the centerline of the (m)-th body,

$$\begin{aligned}\phi_{k,(m)} = \int_{L(m)} d\chi \Big\{ & p_{k,(m)}(\chi)G_{3D}(\chi - x, y - y_m, z) \\ & + q_{k,(m)}(\chi)\frac{\partial}{\partial y}G_{3D}(\chi - x, y - y_m, z)\Big\}\end{aligned} \tag{17}$$

where $p_{j,(m)}$ and $q_{j,(m)}$ are the strengths of three three-dimensional source G_{3D} and dipole $\partial G_{3D}/\partial y$ (Wehausen and Laiton 1960, Eq.13.17 & 13.19). Extracting the two-dimensional singularity, equation (17) can be rewritten as

$$\phi_{k,(m)} = \Lambda(\chi)G_{2D}(y - y_m, z) + \int_{L(k)} d\chi \Lambda(\chi)H(\chi - x, y - y_m, z) \tag{18}$$

where

$$\Lambda(\chi) = p_{k,(m)}(\chi) + q_{k,(m)}(\chi)\frac{\partial}{\partial y} \tag{19}$$

$$H(x,y,z) = G_{3D}(x,y,z) - G_{2D}(y,z) \tag{20}$$

The inner expansion of the far-field solution can be obtained using the Taylor series expansion of the integral term for small y and z (Kim and Sclavounos 1998).

$$\begin{aligned}\phi_{k,(m)} =& \{\Lambda(x)G_{2D}(y-y_m,z)\} + \int_{L(m)} d\chi \Lambda(\chi)H(\chi - x, y_m, 0) \\ &+ \int_{L(m)} d\chi \left(y\frac{\partial}{\partial y} + z\frac{\partial}{\partial z}\right)\Lambda(\chi)H(\chi - x, y_m, z)\mid_{y=y_m,z=0} + O(y^2,z^2)\end{aligned} \tag{21}$$

For the source component, $\partial/\partial y$ becomes zero when $y = 0$. Moreover, when the singularity line is distributed on $z = 0$, equation (21) can be simplified to

$$\begin{aligned}\phi_{k,(m)} =& \left\{p_{k,(m)}(x)G_{2D}(y-y_m,z) + q_{k,(m)}(x)\frac{\partial}{\partial y}G_{2D}(y-y_m,z)\right\} \\ &+ \int_{L(m)} d\chi \left\{p_{k,(m)}(\chi)H(\chi - x, y - y_m, 0)\right\} + O(Kr)\end{aligned} \tag{22}$$

3.3 Matching conditions

Matching two solutions, i.e. equation (15) and (22), leads the following three conditions:

$$\sigma_{k,(m)}(x) + C_{k,(m)}(x)\left\{\sigma_{k,(m)}(x) + \sigma^*_{k,(m)}(x)\right\} = p_{k,(m)}(x) \tag{23}$$

$$\mu_{k,(m)}(x) + C_{k,(m)}(x)\left\{\mu_{k,(m)}(x) + \mu^*_{k,(m)}(x)\right\} = q_{k,(m)}(x) \tag{24}$$

$$\begin{aligned}-C_{k,(m)}(x)d^*_{k,(m)}(x)&\left\{G_{2D}(y-y_m,z) - G^*_{2D}(y-y_m,z)\right\} \\ &= \int_{L(m)} d\chi \left\{p_{k,(m)}(\chi)H(\chi - x, y - y_m, 0)\right\}\end{aligned} \tag{25}$$

Three unknowns, $p_{k,(m)}(x)$, $q_{k,(m)}(x)$, and $C_{k,(m)}(x)$ can be obtained from above three matching conditions.

In deep water, we can simplify the (24) and (25) as

$$\mu_{k,(m)}(x) = q_{k,(m)}(x) \tag{26}$$

$$\begin{aligned}-C_{k,(m)}(x)\sigma^*_{k,(m)}(x)&\left\{G_{2D}(y-y_m,z) - G^*_{2D}(y-y_m,z)\right\} \\ &= \int_{L(m)} d\chi \left\{p_{k,(m)}(\chi)H(\chi - x, y_m, 0)\right\}\end{aligned} \tag{27}$$

In finite depth, the influence of a dipole is more complicated. Especially, in shallow water, a source and a dipole have the same order of the leading terms (Tuck 1970). At a large y where the evanescent modes are ignorable, the wave component of a point dipole in finite depth is written as

$$\frac{\partial}{\partial y}G_{2D}(y,z) \approx sgn(y)\cosh(Kh)\cosh\{K(z+h)\}\frac{K^2 - v^2}{hK^2 - hv^2 + v}e^{-iK|y|} \tag{28}$$

When $K \to 0$,

$$\frac{v}{K} = \frac{K^2 h}{K} \to 0 \tag{29}$$

Using these relations, it is easy to show

$$\frac{\partial}{\partial y} G_{2D}(y,z) \approx sgn(y)\frac{1}{2h} + O(y) \tag{30}$$

The first term in the right-hand side is the potential jump across $y = 0$, which is inversely proportional to the water depth. Lamb (1932, p.72) showed that the potential jump, C, due to a body of its sectional area S in uniform flow between two side hulls is written approximately as

$$C \approx \pm\frac{S}{l} \tag{31}$$

where l is the distance of the transverse boundaries. Since the dipole of its strength $1/2\pi$ can be considered approximately as a circular cylinder of the radius $b = \sqrt{1/2\pi}$, the potential jump becomes

$$C \approx \pm\frac{\pi b^2}{l} = \pm\frac{1}{2l} \tag{32}$$

Therefore, equation (30) is consistent with (32).

The first term in the right-hand side of (30) vanishes in deep water, however, in shallow water, this term plays an important role as a leading-order term. When $K \to 0$, two-dimensional flow due to source and dipole in finite depth show the behaviors similar to uniform flow, i.e. diverging flow by source and uni-directional flow by dipole. Therefore, the antisymmetric component is important as much as the symmetric component. In the present study, the deep and moderate water depths are of interest, so it is assume that this term does not provide a significant contribution.

Associated with source terms, eliminating $C_{k,(m)}(x)$ in (22) and (27) leads to the integral equation for $p_{k,(m)}(\chi)$. The integral equations for deep water and finite depth were introduced by Newman(1978), and Kim and Sclavounos (1998), such that

$$\begin{aligned}\sigma_{k,(m)}(x) = p_{k,(m)}(x) - \frac{1}{2\pi i}\left(1+\frac{\sigma_{k,(m)}}{\sigma^*_{k,(m)}}\right)\left[p_{k,(m)}(\chi)(\gamma+\pi i)\right]+ \\ \int_{L(m)} d\chi\left\{\frac{1}{2}sgn(x-\chi)\ln(2K\mid x-\chi\mid)\frac{\partial}{\partial\chi}p_{k,(m)}(\chi) - \frac{\pi K}{4}R\{K(x-\chi)\}p_{k,(m)}(x)\right\}\end{aligned} \tag{33}$$

for deep water, and

$$\begin{aligned}\sigma_{k,(m)}(x) =& p_{k,(m)}(x) + \frac{\left(Kh/\cosh(Kh)\right)^2}{2iKh}\left(1+\frac{\sigma_{k,(m)}(x)}{\sigma^*_{k,(m)}(x)}\right)\int_{L(m)} d\chi p_{k,(m)}(x-\chi) \\ &\times\left[\frac{1}{2}\frac{K^2}{K^2h - v^2h + v}\left\{-iY_0(K(x-\chi)) + J_0(K(x-\chi)) - \frac{2}{K}\delta(x-\chi)\right\}\right. \\ &\left. - \sum_{n=1}^{\infty}\frac{m_n^2}{m_n^2h + v^2h - v}\left\{\frac{1}{\pi}K_0(m_n(x-\chi)) - \frac{1}{m_n}\delta(x-\chi)\right\}\right]\end{aligned} \tag{34}$$

for finite depth, where

$$R\{x\} = Y_0(x) + 2iJ_0(| x |) + H_0(| x |) \tag{35}$$

and

$$v = \frac{\omega^2}{g} = K\tanh(Kh) = -m_n \tan(m_n h) \tag{36}$$

$Y_0(x)$, $J_0(x)$ and $K_0(x)$ are the Bessel functions of the zero-th order, and $H_0(x)$ is the Struve function. In addition, $\delta(x)$ is the delta function.

$p_{k,(m)}(x)$ can be obtained by solving the integral (34) or (35), and subsequently $C_{k,(m)}(x)$ is computed from

$$C_{k,(m)}(x) = \frac{p_{k,(m)}(x)}{\sigma_{k,(m)}(x) + \sigma^*_{k,(m)}(x)} - \sigma_{k,(m)}(x) \tag{37}$$

The corresponding velocity potential is obtained from (16). Besides, the added mass and damping coefficient are obtained from (7).

The linear equation of motion can be assembled by adding all the linear hydrodynamic forces, inertia and restoring forces, such that

$$\sum_{m=1}^{M}\sum_{k=1}^{6}\Big[\Big(-\omega^2 m_{j,k}^{(n)} + c_{j,k}^{(n)}\Big)\delta_{n,m} - \xi_{k,0}^{(m)}\Big\{\omega^2 A_{j,k}^{(n,m)} - i\omega B_{j,k}^{(n,m)}\Big\}\Big] = X_j^{(n)} \tag{38}$$

for $j = 1,..,6$, and $n = 1,..,M$, where $m_{j,k}^{(n)}$, $c_{j,k}^{(n)}$ and $X_j^{(n)}$ are the mass, restoring force and diffraction force components, respectively. In a typical slender-body theory, two coupled equations of motion are considered; couplings of heave-pitch and sway-yaw-roll. This study concentrates on the heave and pitch motions for the application of unified theory.

4 Validation and application

4.1 Numerical method for strip-theory solution

The two-dimensional strip solution is essential for the application of unified theory. Many numerical methods have been introduced for the two-dimensional boundary value problem, and it is needless to say the details in this paper. The numerical method applied in this study is a boundary integral method (BIM) based on wave Green function. In particular, the computer program of Kim and Sclavounos (1998) has been extended to get rid of the irregular-frequency problem. The solution grids have been distributed inside the body as well as the body surface.

To validate the developed program, the added-mass and damping coefficients have been observed for two semi-submerged circular cylinders. Figure 3 shows two components (n = 1, m = 1 and n = 1, m = 2) and their sum. An adjacent cylinder of the same radius is located at the distance of four times of diameter. Breit and Sclavounos (1986) introduced the total heave added mass and damping coefficients for the same case, and the half of their results can be compared with the sum of two components.

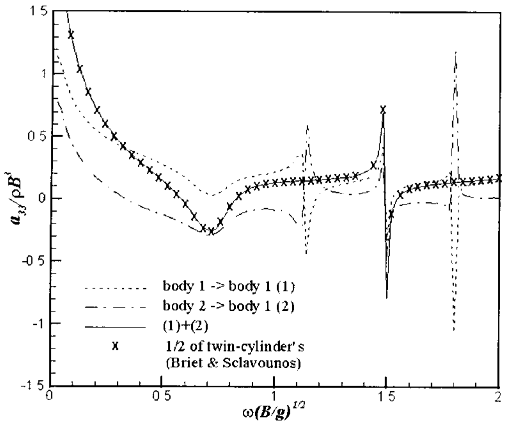

(a) added mass

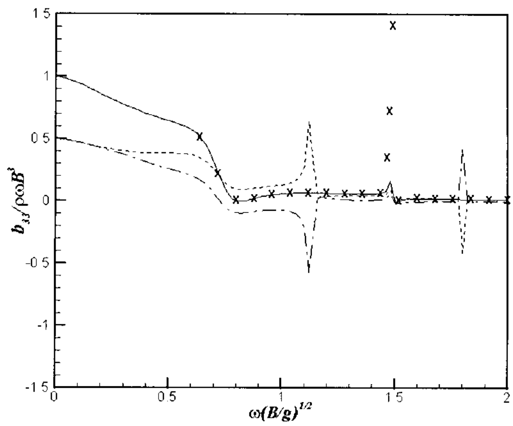

(b) damping coefficient

Figure 3: Components of the sectional heave added-mass ($a_{3,3}$) and damping coefficients ($b_{3,3}$) of two adjacent semi-submerged circular cylinders. $B(diameter)/D(distance) = 4.0$, $a_{3,3}^{(1,1)}$ and $b_{3,3}^{(1,1)}$; dashed line, $a_{3,3}^{(1,2)}$ and $b_{3,3}^{(1,2)}$; dash-dot line, $a_{3,3}^{(1,1)} + a_{3,3}^{(1,2)}$ and $b_{3,3}^{(1,1)} + b_{3,3}^{(1,2)}$; dashed line, half of a twin-cylinder (Breit and Sclavounos 1986); X

In Figure 3, the first resonance can be found near $\omega\sqrt{L/g} = 0.7$. This resonance has a pumping behavior between two bodies, and becomes very complicated when the two bodies are getting closer. Another strong resonance occurs near $\omega\sqrt{L/g} = 1.5$ as the wavelength is close to the distance of free surface between two bodies. Besides these resonances, the sum of two components shows smooth variation, showing a very good agreement with the results of Breit and Sclavounos (1986). However, in the frequency range of Figure 3, two components show another spikes near $\omega\sqrt{L/g} = 1.1$ and 1.8. In particular, the components have opposite signs of change, so that the total quantities are not affected much. At these frequencies, wavelengths are about half ($\omega\sqrt{L/g} = 1.1$) and one and half ($\omega\sqrt{L/g} = 1.8$) of the distance of free surface between two bodies. This results in 180-degree phase difference of two forces, $\partial F_j^{(1)}/\partial\xi_k^{(1)}$ and $\partial F_j^{(2)}/\partial\xi_k^{(1)}$, and consequently two components have opposite trends near these frequencies. The sum of two components is important when the two bodies are connected and moves together, but each component should be considered for independently floating bodies.

4.2 Two adjacent slender ships

For the application of the present theory to three-dimensional problems, it is necessary to divide the strip solution into symmetric and anti-symmetric components. In particular, the symmetric component is more important in the present approach to obtain $C_{k,(m)}$ and consequently the complete near-field solution. To minimize numerical effort for the decomposition, this study approximates the symmetric component to the single-body solution. This approximation is valid when the other bodies are not very close. The symmetric component can be decomposed further into a component due to the single body under unit-amplitude motion and an additional component due

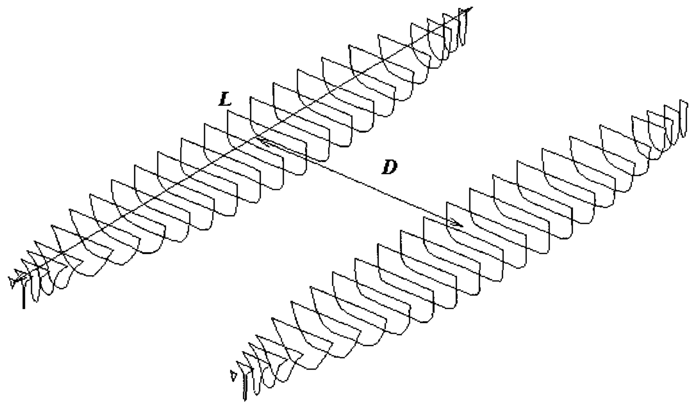

Figure 4: Two adjacent Series 60 hulls; computational sections

to the existence of other body. In general, the single-body component is dominant. This concept is similar to the method of Breit and Sclavounos (1986) for catamaran. However, it is obvious that the current approximation has the limitation in considering the dipole behavior.

Numerical test has been carried out for two adjacent Series 60 hulls of the block coefficient 0.7. Figure 4 shows the strip sections of the two Series 60 hulls. Each ship has been represented with 23 sections and about 30 segments per section. To get rid of irregular frequencies, three pseudo panels have been added inside each section.

Figure 5 shows the heave and pitch added-mass and damping coefficients for $D/L = 0.2$. This figure compares the solutions of three methods; slender-body theory (SBT) without $C_{k,(m)}(x)$ correction, (i.e. strip solution) and with correction (i.e. unified theory), and a three-dimensional panel method. The agreement between unified theory and the three-dimensional method is fair, while the accuracy of strip method becomes poor at low frequency, as expected. A peak is found near $\omega\sqrt{L/g} = 3.0$, and this is the first resonance described in Figure 3. This resonance effect becomes stronger as the gap between two ships are closer, and wave run-up as well as interaction force is an important factor for ship design. The position of peak predicted by unified theory shows a slight difference with the three-dimensional solution, and this is due to the lack of considering the influence of other body, especially missing antisymmetric component. This is the limitation of the present approximation.

This computation has been carried out using a PC equipped with a Pentium 4 process of 1.4 GHz. For a single wave frequency, it took about 2-3 seconds to obtain the unified theory solution and faster for strip method, while about 3 minutes for the three-dimensional method.

The heave added-mass and damping coefficients for different water depths are shown in Figure 6. Figure (a) and (b) are the diagonal terms, i.e. $m = n = 1$, and both the added-mass and damping coefficients show the same trend with the single-body problem (Kim and Sclavounos 1998). However, at very low frequencies, the present method does not provide reliable solutions for the off-diagonal terms, i.e. $m = 2$ and $n = 1$, particularly for wave damping. As explained above, this is due to the shallow-depth effects of the anti-symmetric modes. Although the diagonal components look fine as the symmetric mode is dominant, but the same accuracy cannot be expected for the off-diagonal components when $K \to 0$.

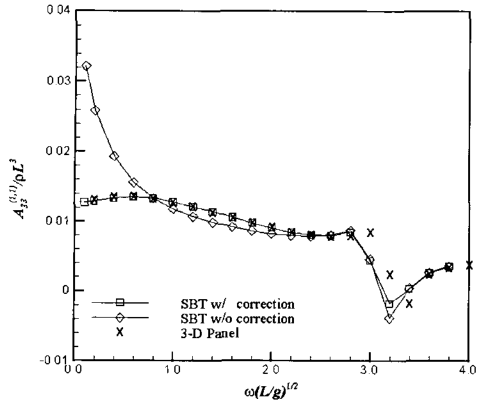

(a) $A_{3,3}^{(1,1)}$

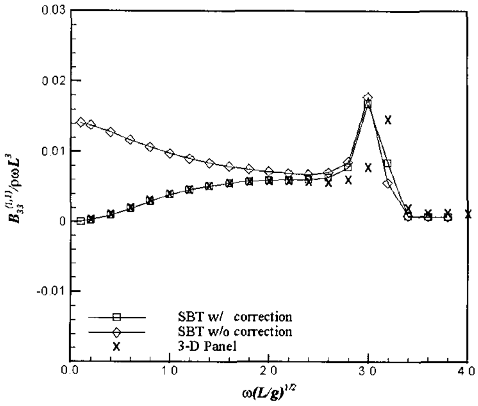

(b) $B_{3,3}^{(1,1)}$

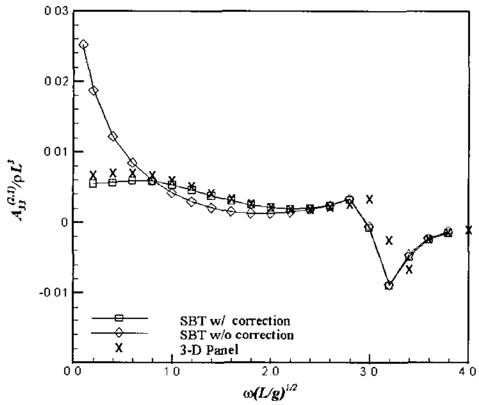

(c) $A_{3,3}^{(2,1)}$

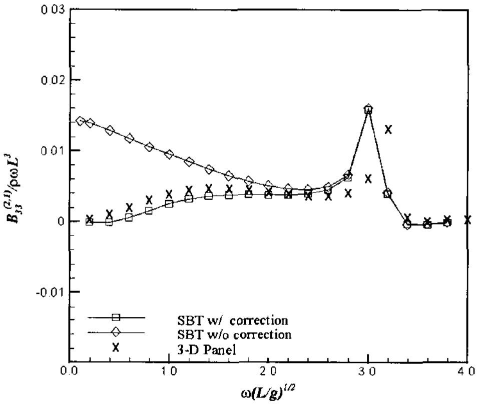

(d) $B_{3,3}^{(2,1)}$

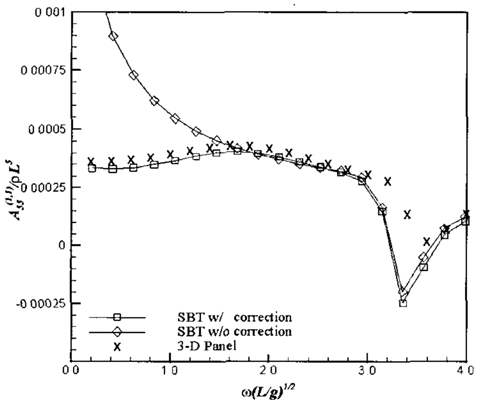

(e) $A_{5,5}^{(1,1)}$

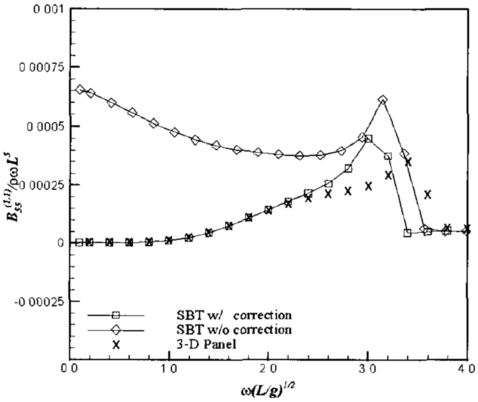

(f) $B_{5,5}^{(1,1)}$

Figure 5: Hydrodynamic coefficients of the Series 60 hull with an adjacent ship (see Figure 6); $D/L = 0.2$, $D/B = 1.37$, with (unified) and without (strip) $C_{k,(m)}(x)$ correction.

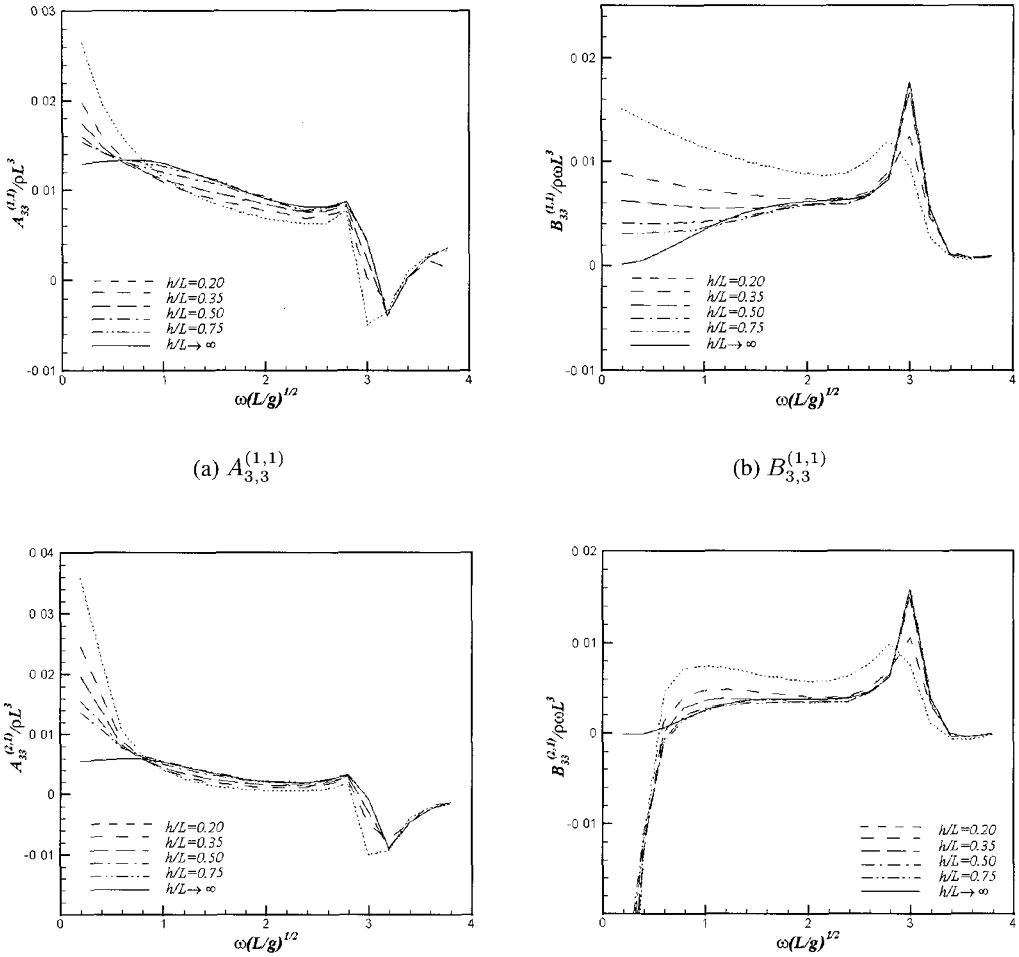

(a) $A_{3,3}^{(1,1)}$ (b) $B_{3,3}^{(1,1)}$

(c) $A_{3,3}^{(2,1)}$ (d) $B_{3,3}^{(2,1)}$

Figure 6: Depth effects on heave added-mass and damping coefficients; two Series 60 hull, $D/L = 0.2$, $D/B = 1.37$

4.3 Multimaran - Single-Body Approach

The present method is also useful for multimarans. For instant, a catamaran can be considered as a particular case of the previous application for two bodies. Recently, ships with more than two bodies, e.g. trimaran and pentamaran, are of great interest for both military and commercial purposes. In general, these ships have multiple sidehulls much smaller than the main body. Furthermore, the distance between the main body and the sidehulls is the order of ship beam.

The present study has been extended to the seakeeping problem of trimaran ships, although the forward speed is not considered. In particular case that all bodies are moving together and the sidehulls are close to the main body, it is not necessary to solve the sub problems to obtain individual interaction components. Treating all the sections as a part of one single ship (not a

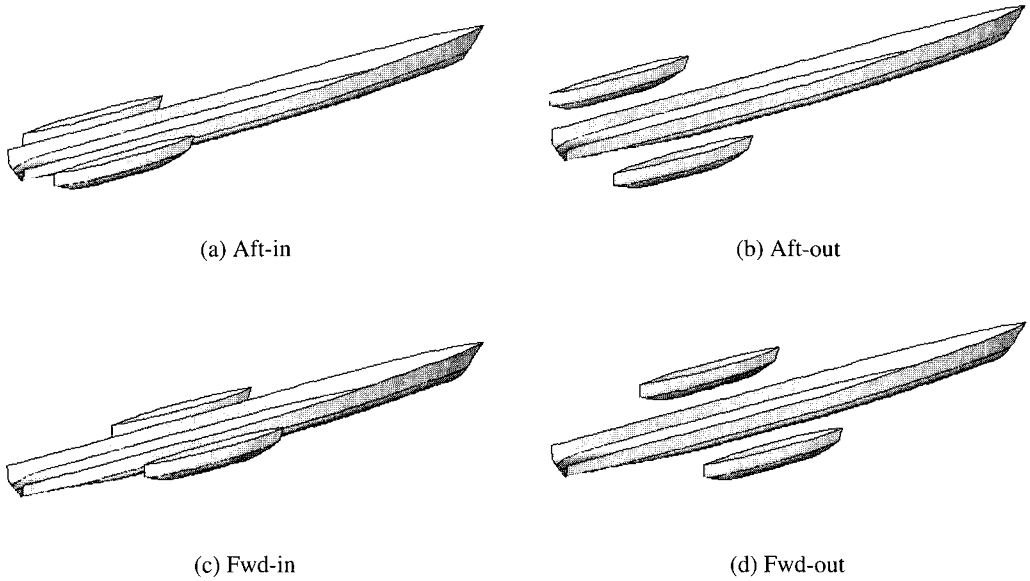

Figure 7: Four models of trimaran

single body) is more efficient than computing all components. Figure 7 shows four trimaran ships with the sidehulls of different longitudinal and transverse locations (Harris 1999, Kim and Weems 2000). The present method has been applied to the prediction of the hydrodynamic coefficients and motion RAOs of these ships. The computation has been carried out for a light load condition which the ship length of load waterline, beam and draft are 128.27 m, 9.75 m and 4.5 m, for the main hull, and 36.17 m, 2.80 m, and 2.74 m for one sidehull. The combinations of two longitudinal (fwd and aft) and two transverse (in- and out-board) positions for the sidehulls are considered. Especially, the distance between the centerlines of the main hull and the inboard and outboard sidehulls are 9.75 m and 19.51 m, respectively.

The heave added-mass and damping coefficients of the aft-out mode (Figure 7(b)) are plotted in Figure 8, showing the comparison with the three-dimensional panel method. As expected, the agreement is excellent. Figure 9 shows the heave and pitch added-mass and damping coefficients of the four models. From this figure, it is observed that both the transverse and longitudinal locations of the sidehulls are important. The heave force seems more sensitive to the transverse position of the sidehulls rather than the longitudinal position. This indicates that the wave resonance between the main hull and the sidehulls plays an important role in the heave force. On the other hand, the pitch added-mass and damping coefficients are significantly sensitive to the longitudinal position. Owing to larger moment arm, the pitch moment of the aft-sidehull trimaran is more sensitive to a change of the heave force than the fwd-sidehull trimarans. This sensitivity is obvious in figure (c) and (d).

This computation has been extended to the motion RAOs. The wave excitation forces and moments have been obtained using a far-field Haskind relation. Sclavounos (1985a) suggested the far-field formula for the diffraction force on a slender body, and Breit and Sclavounos (1986) introduced a rational approach to approximate the solution of diffraction problem using a technique

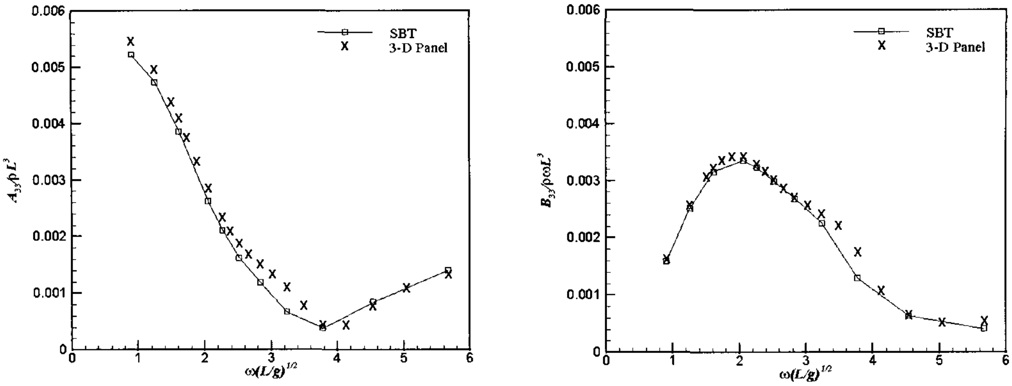

(a) Heave added-mass (b) Damping coefficients

Figure 8: Heave added-mass and damping coefficients; comparison with three-dimensional panels results, aft-out arrangement

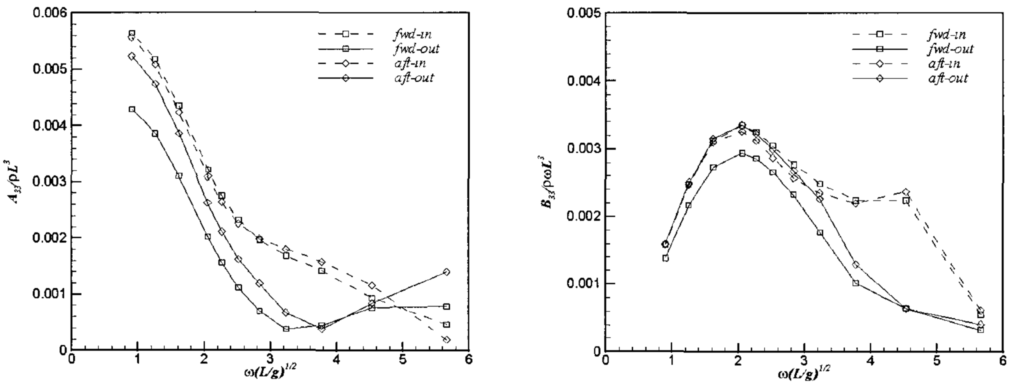

(a) $A_{3,3}$ (b) $B_{3,3}$

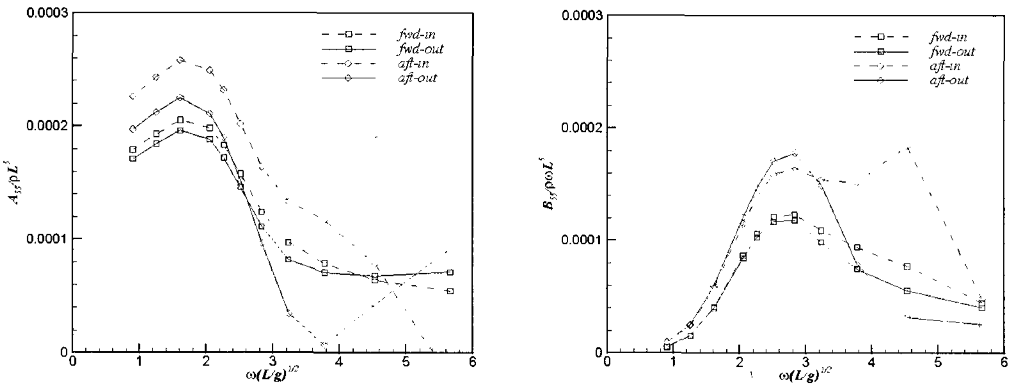

(c) $A_{5,5}$ (d) $B_{5,5}$

Figure 9: Hydrodynamic coefficients of four trimaran models

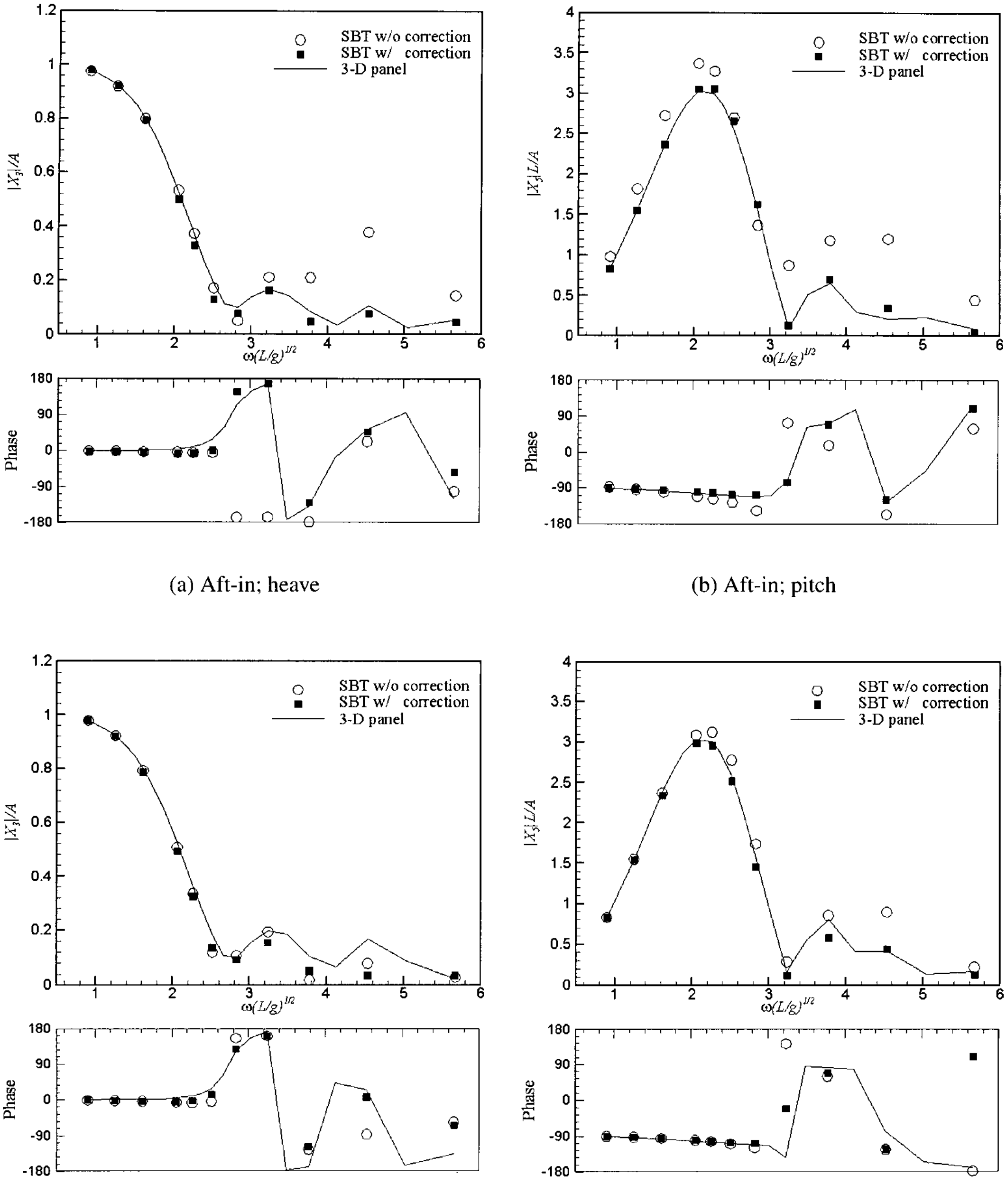

(a) Aft-in; heave

(b) Aft-in; pitch

(c) Aft-out; heave

(d) Aft-out; pitch

Figure 10: Heave and pitch motion RAOs and phases; aft-outrigger trimaran

similar to the radiation problem. Besides, Kim and Sclavounos (1997) showed that the far-field formula provides more accurate excitation forces and moments than the near-field Haskind relation in the application of slender-body theory.

Figure 10 shows the heave and pitch RAOs at head sea. The agreement of the motion RAOs between unified theory and the three-dimensional panel method is fair. The agreement of phase difference is also excellent. In this problem, strip theory overpredicts the motion RAOs, especially for the trimarans with the in-board sidehulls. Therefore, the application of strip theory for multi-hull ships is not reliable as much as for mono-hull ships.

5 Summary

In the present study, unified theory has been extended for the radiation problem of multi floating bodies. The linear radiation force on each body has been decomposed into as many as the number of the bodies, and the sub-problem has been solved for each component. The unified theory for the mono-hull problem has been extended for each sub-problem. The application models are adjacent Series 60 hulls and trimarans. The added-mass and damping coefficients have been compared with the results of a three-dimensional panel method, showing a good agreement. It has been found that the present theory is not valid in very shallow water, but the unified theory provides reliable and accurate solutions in overall frequency range for deep water and not extremely shallow depth.

References

BAI, K.J. AND YEUNG R.W. 1974 Numerical solutions to free surface problems. Proc. 10th Symposium on Naval Hydrodynamics, Arlington, VA, pp. 609-648

BORRESEN, R. 1984 The unified theory of ship motions in water of finite depth, Ph.D. Thesis, The Norwegian Institute of Technology

BREIT, S.B. AND SCLAVOUNOS, P.D. 1986 Wave interaction between adjacent slender bodies. J. of Fluid Mechanics, **165**, pp. 273-296

EMMERHOFF, O.J. AND SCLAVOUNOS, P.D. 1996 The slow-drift motion of arrays of vertical cylinders. J. of Fluid Mechanics, **242**, **31**, pp. 31-50

FANG, M.C. AND KIM, C.H. 1986 Hydrodynamically coupled motions of two ships advancing in oblique waves. J. of Ship Research, **30**, pp. 159-171

FRANK, W. 1967 Oscillation of cylinders in or below the free surface of deep fluids, Report 2375, David W. Taylor Naval Ship Research and Development Center

HARRIS, N. 1999 Effective horsepower and seakeeping tests on a trimaran model. Report EW-01-99, United States Naval Academy, Annapolis, MD.

KAGEMOTO, H. AND YUE, D.K.P. 1985 Wave forces on multiple leg platforms. Proc. BOSS '85, Delft, The Netherlands, pp. 751-762

KASHIWAGI, M. 1993 Heave and pitch motions of a catamaran advancing in waves. Proc. FAST'93, Yokohama, Japan, pp. 648-655

KIM, C.H. AND FANG, M.C. 1985 Vertical relative motion between two longitudinally parallel adjacent platforms in oblique waves. Proc. 4th OMAE, **1**, pp. 114-124

KIM Y. AND SCLAVOUNOS P.D. 1997 The computation of the second-order hydrodynamic forces on a slender ship in waves. Proc. 12th International Workshop on Water Waves and Floating Bodies, Marseuille, France, pp. 139-142

KIM, Y. AND SCLAVOUNOS, P.D 1998 A finite-depth unified theory for linear and second-order problems of slender ships. J. of Ship Research, **42**, pp. 297-306

KIM, Y. AND WEEMS, K. 2000 Motion responses of the high-speed crafts in regular and random waves. Proc. RINA, High-Speed Craft Conference for wake-wash & Motion control, London, UK.

KIM, Y. 2000 Computation of the linear and nonlinear hydrodynamic forces on slender ships with zero speed in waves: infinite-depth case. J. the Society of Naval Architects of Korea, **37**, pp. 1-13

KORVIN-KROUKOVSKY, B.V. 1955 Investigation of ship motions in regular waves, Trans. SNAME, English Trans. , **85**, pp. 590-632

LAMB, H. 1932 Hydrodynamics. Dover, New York

LEE, C.M. 1976 Theoretical prediction of motion of small-waterplane-area, twin-hull (SWATH) ships in waves. Report 76-0046, David W. Taylor Naval Ship Research and Development Center.

LIN, W.M. AND YUE, D.K.P. 1990 Numerical solutions for large-amplitude ship motions in the time-domain. Proc. 18th Symposium on Naval Hydrodynamics, Ann Arbor, MI, pp. 41-66

MANIAR, H.D. AND NEWMAN, J.N. 1997 Wave diffraction by a long array of cylinders. J. of Fluid Mechanics, **339**, pp. 309-330

NAKOS, D.E., KRING, D.G., AND SCLAVOUNOS, P.D. 1993 Rankine panel methods for transient free surface flows. Proc. 6th Numerical Ship Hydrodynamics, Iowa City, IA, pp. 613-634

NEWMAN, J.N. 1978 The theory of ship motions. Advanced Applied Mechanics, **18**, pp. 221-283

NEWMAN, J.N. AND SCLAVOUNOS, P.D. 1980 The unified theory for ship motions. Proc. 13th Symposium on Naval Hydrodynamics, Tokyo, Japan, pp. 1-22

OGILVIE, T.F. AND TUCK, E.O. 1969 A rational strip theory of ship motions. Part I, Report-013, Dept of Naval Architecture and Marine Engineering, University of Michigan

OHKUSU, M. 1974 Hydrodynamic forces on multiple cylinders in waves. Proc. International Symposium in the Dynamics of Marine Vehicles and Structures in Waves, Institute of Mechanical Engineers, pp. 107-112

PRUDNIKOV, A.P., BRYCHKOV, Y.A. AND MARICHEV, O.I. 1986 Integrals and Series.**1**. Grodon and Breach Science Publishers, New York

SALVESEN, N., TUCK, E.O. AND FALTINSEN, O.M. 1970 Ship motions and sea loads. Trans. SNAME, **78**, pp. 250-287

SCLAVOUNOS, P.D. 1984 The diffraction of free-surface waves by a slender ships. J. of Ship Research, **28**, pp. 29-47

SCLAVOUNOS, P.D. 1985a Forward speed vertical wave exciting forces on ships in waves. J. of Ship Research, **29**, pp. 105-111

SCLAVOUNOS, P.D. 1985b Users Manual of NIIRID: a general purpose program for wave-body interactions in two dimensions. Dept. of Ocean Engineering, MIT.

SPRING, B.H. AND MONKMEYER, P.L. 1974 Interaction of plane waves with vertical cylinders. Proc. 14th International Conference on Coastal Engineering, chapter **107**, pp. 1829-1845

TUCK, E.O. 1970 Ship motions in shallow water. J. of Ship Research, **14**, pp. 317-328
WEHAUSEN, J.V. AND LAITONE, E.V. 1960 Surface waves. Handbuch der Physic, **9**, pp. 446-778